

Numerical forecasts for lab experiments constraining modified gravity: the chameleon model

Sandrine Schlögel*

*naXys, University of Namur,
Rempart de la Vierge 8, Namur, 5000, Belgium*

**E-mail: sandrine.schlogel@unamur.be
www.unamur.be*

*Centre for Cosmology, Particle Physics and Phenomenology, Institute of Mathematics and
Physics, Louvain University, Chemin du Cyclotron 2, 1348 Louvain-la-Neuve, Belgium*

Sébastien Clesse

*naXys, University of Namur,
Rempart de la Vierge 8, Namur, 5000, Belgium*

*Institute for Theoretical Particle Physics and Cosmology (TTK), RWTH Aachen University,
D-52056 Aachen, Germany*

André Füzfa

*naXys, University of Namur,
Rempart de la Vierge 8, Namur, 5000, Belgium*

**E-mail: sandrine.schlogel@unamur.be
www.unamur.be*

*Centre for Cosmology, Particle Physics and Phenomenology, Institute of Mathematics and
Physics, Louvain University, Chemin du Cyclotron 2, 1348 Louvain-la-Neuve, Belgium*

Current acceleration of the cosmic expansion leads to coincidence as well as fine-tuning issues in the framework of general relativity. Dynamical scalar fields have been introduced in response of these problems, some of them invoking screening mechanisms for passing local tests of gravity. Recent lab experiments based on atom interferometry in a vacuum chamber have been proposed for testing modified gravity models. So far only analytical computations have been used to provide forecasts. We derive numerical solutions for chameleon models that take into account the effect of the vacuum chamber wall and its environment. With this realistic profile of the chameleon field in the chamber, we refine the forecasts that were derived analytically. We finally highlight specific effects due to the vacuum chamber that are potentially interesting for future experiments.

Keywords: modified gravity; lab experiment; dark energy

1. Introduction

A challenging issue in cosmology today consists in explaining the current accelerated cosmic expansion or 'dark energy'. Even if the standard model of cosmology reproduces current observations, the cosmological constant can not explain the coincidence issue and faces a fine-tuning problem. The most simple alternative is to introduce a dynamical scalar field, potentially originating from the gravity sector. However, such models are a dangerous business since they have to pass stringent constraints in the Solar system and in lab experiments. To do so, models invoking

a screening mechanism, like the chameleon^{1,2}, have been built: in dense environment like the Solar system, the scalar field is suppressed while it acts on sparse environment, like in the cosmos at late time.

Recently, a new lab experiment based on atom interferometry with a test mass inside a vacuum chamber has been designed for testing modified gravity models³. The idea is that, even if their nuclei appear to be dense, atoms are so small that the scalar field is unsuppressed. Additional acceleration on individual atoms due to the chameleon field gradient inside the vacuum chamber in the presence of the test mass could be measured. Analytical calculations derived so far in Refs. 3, 4 show that most of the chameleon parameter space is constrained by such an experiment.

Nevertheless, the authors assumed that the wall effect is negligible and the value of the scalar field at the center of the chamber is then determined as a function of the size of the chamber^{3,4}. We provide numerical computations with the following minimal assumption⁵: the chameleon field reaches its equilibrium value ϕ_∞ in the outside atmosphere. Our results reveal that the scalar field amplitude inside the chamber is related to ϕ_∞ instead of the chamber size, in the case where the test mass perturbs weakly the chameleon profile. We also study the *strongly* perturbing case where *thin shell* appears. In both cases, we provide forecasts for the acceleration due to the scalar field a_ϕ which is related to the scalar field gradient inside the vacuum chamber, experimental constraint³ being $a_\phi/g < 5.5 \times 10^{-7}$, with g the Earth gravitational acceleration. We also highlight the effects of the test mass density and size, a result which can be interesting for designing further experiments.

2. The chameleon model

In this section, we briefly remind the chameleon model. We start from the general scalar-tensor theory action written in the Einstein frame,

$$S = \int d^4x \sqrt{-g} \left[\frac{R}{2\kappa} - \frac{1}{2} (\partial\phi)^2 - V(\phi) \right] + S_m [A^2(\phi) g_{\mu\nu}; \psi_m], \quad (1)$$

with R , the scalar curvature, $\kappa = 8\pi/m_{\text{pl}}^2$, m_{pl} being the Planck mass, ψ_m the matter fields, $V(\phi)$ the chameleon potential (in the following, we will consider $V(\phi) = \Lambda^{\alpha+4}/\phi^\alpha$, α and Λ being the parameters of the potential) and $A(\phi)$ a general coupling function (in the following, we will consider $A(\phi) = e^{\phi/M}$, M being a parameter). For a static and a spherically symmetric spacetime in the non-relativistic limit, the Klein-Gordon equation is given by,

$$\phi'' + \frac{2}{r}\phi' = \frac{dV_{\text{eff}}}{d\phi}, \quad \frac{dV_{\text{eff}}}{d\phi} = \frac{dV}{d\phi} + \tilde{\rho} A^3 \frac{dA}{d\phi}, \quad (2)$$

with V_{eff} the effective potential, $\tilde{\rho}$ the density written in the Jordan frame⁶ such as it obeys to the energy conservation $\nabla_\mu \tilde{T}^{\mu\nu} = 0$, a prime denoting a derivative with respect to the radial coordinate. The effective potential minimum ϕ_{min} is given by,

$$\phi_{\text{min}} = \left(\frac{\alpha \Lambda^{\alpha+4} M}{\tilde{\rho}} \right)^{1/(\alpha+1)}, \quad (3)$$

in the limit $A(\phi) \approx 1$. Depending on the environment, the scalar field is suppressed (dense environment) or not (sparse environment).

3. Numerical results

In order to constrain the acceleration due to the scalar field $a_\phi = \partial_r \phi / M$, we solve the Klein-Gordon equation inside the test mass, the vacuum chamber, the wall and in the air outside the vacuum chamber with the minimal assumptions: the scalar field reaches its equilibrium value $\phi_\infty = \phi_{\min}(\tilde{\rho}_{\text{air}})$ at spatial infinity and the solution should be regular at the origin of coordinates and everywhere continuous. We use a solver for multi-point boundary value problem with unknown parameters⁷, the boundary conditions being given by $\phi'(r=0) = 0$ and a Yukawa profile far in the exterior environment,

$$\phi = \phi_\infty + \frac{\mathcal{C}e^{-\mathcal{M}r}}{r}, \quad (4)$$

with $\mathcal{M} = d^2V_{\text{eff}}/d\phi^2|_{\phi=\phi_\infty}$, the constant of integration \mathcal{C} being a parameter to be determined by the numerical algorithm.

3.1. Acceleration forecasts

We compare the numerical and analytical profiles of the scalar field and the acceleration on Fig. 1 for various M ($\alpha = 1$ and corresponding Λ being obtained from the cosmological constraints coming from SNe Ia observations⁶). The numerical results differ by up to one order of magnitude for the acceleration compared to previous analysis^{3,4}, indicating that the effect of the wall cannot be neglected in a precise investigation of the chameleon parameter space. Indeed, varying the wall density by two orders of magnitude (see dotted lines on the scalar field profile of Fig. 1), we show that the wall perturbs more or less importantly the field profile. The effect remains however negligible for the acceleration profile that is related to the gradient of the field. Another important result is the determination of the central value of the scalar field: in Ref. 4, it is given by the size of the chamber while the numerical simulations show that it is better approximated by $\phi_\infty = \phi_{\min}(\tilde{\rho}_{\text{air}})$. On Fig. 2, we study the effect of α and M on the acceleration at 8.8 mm far from the test mass (refers as the *near* position in Ref. 3) where the acceleration is measured experimentally. We conclude that the experiment presented in Ref. 3 is able to rule out the chameleon model presented in the previous section for $M \lesssim 10^{17}$ GeV whatever α . Discrepancies due to α in the determination of the acceleration highlighted on Fig. 2, appears when the limit $|A(\phi) - 1| \ll 1$ is no more valid. We also studied the thin shell regime and our results validate the analytical approximations to a good accuracy.

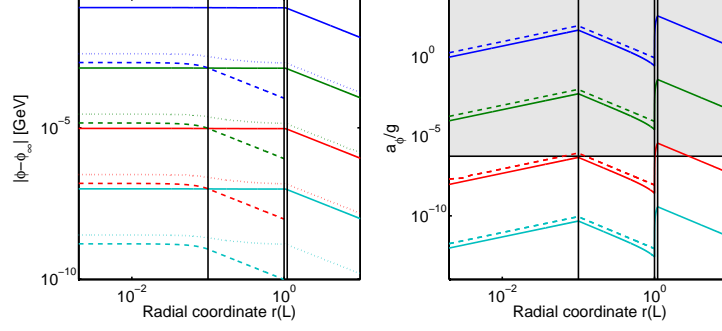


Fig. 1. Scalar field $|\phi - \phi_\infty|$ and acceleration a_ϕ profiles ($\alpha = 1$ and $\Lambda = 2.6 \times 10^{-6}$ GeV) for various M ($M = 10^{13}, 10^{15}, 10^{17}, 10^{19}$ GeV in blue, green, red and light blue). Solid and dashed lines refer to numerical (4 regions) and analytical (2 regions) profiles respectively while dotted lines are obtained when lowering the wall density by a factor 10^2 . The vertical lines mark out the four regions (test mass, vacuum chamber, chamber wall and outside)⁵.

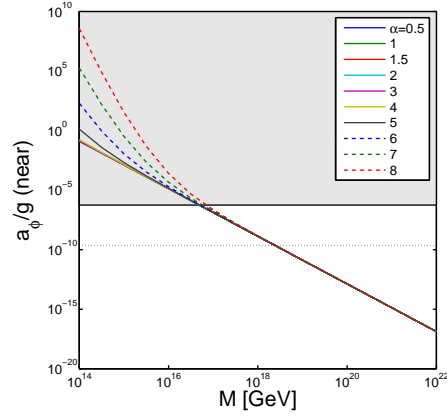


Fig. 2. Forecast for the normalized acceleration a_ϕ/g measured in the *near* position, i.e. 8.8 mm far from the test mass, for various M and α . Dotted line represents the acceleration due to the gravitational interaction with the test mass. The gray rectangle shows which part of the parameter space is ruled out⁵.

3.2. Geometry effects

As stated in the Sec. I, in the case where the scalar field is *weakly* perturbed by the test mass, we observe only a small deviation with respect to ϕ_∞ . This is due to the presence of the wall chamber. It stabilizes the scalar field and gives it a kick for reaching ϕ_∞ . Furthermore, on Fig. 1, we see that the wall density is responsible

for a variation of two orders of magnitude in the scalar field profiles. Since in the experimental setup proposed in Ref. 3 the wall and test mass are similar in size and density, we expect similar effects while varying test mass density and size. The acceleration profiles for the test mass made of aluminum and tungsten with a radius of 5 mm, 1 cm and 3 cm are reported on Fig. 3. We show that, choosing a test mass which is denser and bigger, the acceleration can differ by almost a factor 10.

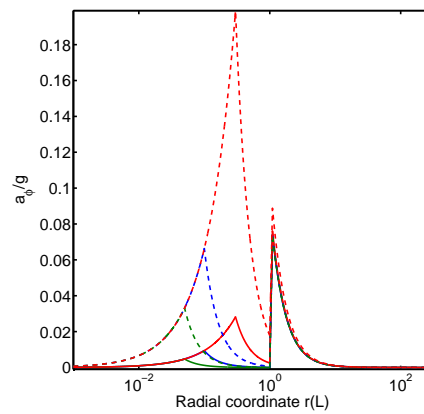


Fig. 3. Comparison of chameleon acceleration a_ϕ/g depending on which material the test mass is made of. Solid and dashed lines correspond to aluminum and tungsten ρ_A respectively while green, blue and red colors correspond to 5 mm, 1 cm and 3 cm test mass radius. We fix here $\alpha = 1$ and $M = 10^{15}$ GeV.

4. Conclusion

We derived numerically forecasts for the experiment of Ref. 3 for various chameleon models in the *weakly perturbing regime*. We showed that analytical and numerical acceleration forecasts and constraints differ by up to one order of magnitude. We also highlight that the numerical simulations can be helpful for precise investigation of the parameter space of the chameleon models as well as for optimizing the experimental setup. The same numerical method has been used to derive constraints on other chameleon potentials in Ref. 5 for the thin shell regime. Our numerical method could be easily extended to other modified gravity models like the symmetron.

Acknowledgments

We warmly thank Holger Müller for the discussion during the MG meeting and the following conversation where Justin Khoury, Benjamin Elder and Philipp Haslinger took part. We also warmly thank Clare Burrage and Christophe Ringeval for useful comments and discussion. S.S. is supported by the FNRS-FRIA, S.C. is partially

supported by the *Return Grant* program of the Belgian Science Policy (BELSPO) and A. F. is partially supported by the ARC convention No. 11/15-040.

References

1. J. Khoury, A. Weltman, *Phys.Rev.Lett.* **93**, 171104 (2004).
2. J. Khoury, A. Weltman, *Phys.Rev.* **D69**, 044026 (2004).
3. P. Hamilton, M. Jaffe *et al.*, *Science*, **349**, 849-851 (2015)
4. C. Burrage, E. J. Copeland, E. Hinds, *JCAP* **1503**, 042 (2015).
5. S. Schlögel, S. Clesse and A. Füzfa, [arXiv:1507.03081](#) *Probing Modified Gravity with Atom-Interferometry: a Numerical Approach*, 2015.
6. A. Hees and A. Füzfa, *Phys.Rev.* **D85**, 103005 (2012).
7. L.F. Shampine, I. Gladwell, and S. Thompson, *Solving ODE's with Matlab* (Cambridge University Press, 2003).